NTNU – Trondheim
Norwegian University of
Science and Technology

Active matter

Collective Motion due to Quincke Rotation

Tommy Fjelde Kristiansen

Master of Science in Physics and Mathematics
Submission date: July 2015
Supervisor: Jon Otto Fossum, IFY
Co-supervisor: Paul Dommersnes, IFY

Norwegian University of Science and Technology
Department of Physics

Active Matter: Collective motion due to Quincke rotation

Tommy Fjelde Kristiansen

June 2015

PROJECT / MASTER THESIS

Department of Physics

Norwegian University of Science and Technology

Supervisor 1: Jon Otto Fossum

Supervisor 2: Paul Dommersnes

Preface

Master thesis in soft and complex matter at the institute of physics at NTNU as part of the study programme Physics and Mathematics. The thesis is in part based on prior experiments carried during the master project in autumn 2014, but the main work was done during the spring semester of 2015. The idea for this project was brought up by prof. Jon Otto Fossum and prof. II Paul Dommersnes when discussing a related project being undertaken by phD candidate Alexander Mikkelsen. It is assumed that the reader posses some understanding of electrodynamics, hydrodynamics and stability analysis, but while preferable it should hopefully not be strictly necessary.

Trondheim, 2012-12-16

(Your signature)

Tommy Fjelde Kristiansen

Acknowledgment

I would like to thank my supervisors prof. Jon Otto Fossum and prof. II Paul Gunnar Dommersnes for their patience, guidance and sage advice provided over the course of my master thesis. A special thanks goes to Phd candidate Aleksander Mikkelsen, for providing logistical support, and more importantly, answering all the questions to embarrassing to ask the supervisors. I am grateful for the discussions we had with Dr. Jakko Timonen during his visit during Nordic Physics Day. It was Dr. Jakko Timonen who pointed out the inclined cell trick to determine the degree of pinning in the cell. Some of the images in this report were provided by the courtesy of prof. II Paul Gunnar Dommersnes, these have been highlighted.

T.F.K

(Your initials)

Summary and Conclusions

This thesis investigates Quincke induced collective motion. It is mostly a qualitative study, but it attempts to connect Quincke induced collective motion to the field of active matter as a whole. The thesis has two objectives. Firstly it shall attempt to create an system in which collective behaviour of Quincke rotors can be investigated. Secondly it attempts to gather qualitative data from this system, and compare it with relevant sources. It is concluded that the experiment is a partial success. The system used manages to produce living crystals, but deviates from other sources when dealing with vortex formation. Both are forms of collective behaviour.

Contents

Preface i

Acknowledgment ii

Summary and Conclusions iii

1 Introduction **2**

1.1 Background 2

1.2 Objectives 5

1.3 Limitations 6

1.4 Approach 6

1.5 Structure of the Report 7

2 Theory **8**

2.1 Active matter 8

2.1.1 The Vicsek Model 8

2.2 Quincke induced collective motion 10

2.2.1 Single Quincke Roller 10

2.2.2 Interaction with other particles 14

3 Methods and Procedures **16**

3.1 Set-up 16

3.2 Methods 17

3.3 Preparation and cleaning 17

3.4 Weaknesses and Limitations 18

4 Results **20**

4.1 Active turbulence 20

4.2 Vortex formation 20

4.3 Living Crystals 22

5 Summary **29**

5.1 Summary and Conclusions 29

5.2 Discussion 30

5.3 Recommendations for Further Work 30

Bibliography **31**

Chapter 1

Introduction

1.1 Background

Collective motion, often observed as flocking, is commonly observed phenomenon in nature. The term collective motion refers to the synchronized motion of interacting individuals in a group. The most common examples range from schools of fish, flocks of birds to insect swarms and pedestrians, see Fig. 1.1. Smaller organisms, such as cells and bacteria, is also known to undergo collective motion[5] [12] [16].

Similar collective behaviour have recently been found in driven "non-living" systems. Examples include granual rods[9], and elongated particles on vibrating surfaces [1], self-propelled gold colloids driven by surface chemical reactions[18] and electro-hydrodynamic propulsion of PMMA beads[2]. The variety of systems demonstrating similar behaviour, hints toward underlying universal rules for collective motion and flocking dynamics. It is the search for these underlying rules that provides the motivation for investigating collective behaviour in general.

When describing the flocking dynamics for systems that can be both living and non-living, it becomes useful to introduce the concept of active matter. Active matter, as opposed to passive matter, is defined as a system of active units that can consume energy to perpetuate motion. Because of their energy consuming nature, active systems operate outside of thermal equilibrium. A key feature of active matter, is that the direction of movement is not determined by outside acting forces. Conversely, passive systems depends on the external force to determine the direction of movement. Other useful terminology includes active turbulence, vortices and living

crystals. Active turbulence refers to turbulent dynamics due to active units moving through a medium. Vortices are spiral like motions that can be either stationary or moving. Recently it was discovered that swimming bacteria and self-propelled colloidal particles may form "'living crystals"'[13][11]. Living crystals refers to crystal like structures, that are capable of forming, breaking down and then reform somewhere else.

Figure 1.1: Examples of collective motion. 1. Flock of birds, picture taken from http://www.pacificnorthwestbirds.com 2. School of fish, picture taken from http://i.huffpost.com. 3. Swarm of butterflies, picture taken from http://static1.squarespace.com . 4. Pedestrians, picture taken from http://www.rudi.net .

Problem Formulation

This study focuses on the induced collective motion of spherical particles due to an electro-hydrodynamic phenomenon called Quincke rotation[14]. The Quincke rotation provides the propulsion mechanism that turns a system of inanimate spherical particles into active matter. Areas of particular interest includes forms of collective motion that can be described as active turbulence, vortex formation and living crystals. The set-up being used for this experiment is an interesting one, as it displays a wide variety of different forms of collective motion. Studying this system could therefore provide some insight into the fundamental rules dictating collective motion, or serve as a stepping stone for further experiments.

Literature Survey

Most of the scientific literature regarding active matter and collective motion is recent, however the idea of providing a framework to describe this kind of group behaviour is not new. In his paper on simulated flocks in computer graphics, Reynolds [15] (1987) presents three abstract rules for collective motion in flocks.

- Collision avoidance, avoiding collision within the flock
- Velocity matching within the flock, including direction and speed
- Centring, flock members desiring to stay close to the centre of the flock

Using these rules, it is possible to create a systems that demonstrates collective motion for active matter. By using boids as a generalized agent, he is able to reproduce bird flocking behaviour. Later on, Vicsek et al. [22] was able to create a model for flocking behaviour in a particle system. The Vicsek Model, as it has later been referred to, relies on particles assuming the average velocity of their neighbouring particles with some added random perturbation.

In their article Toner and Tu [19] presents an quantitative theory for flocking, primarily for boids and birds. Their model, drawing inspiration from Reynolds [15] and Vicsek et al. [22], focuses on long term and long range flock behaviour within the flock[1].

Guillaume and Chaté [7] building on the work of Vicsek et al. [22], discovers that the onset of collective motion is always discontinuous with respect to vectorial noise[2]. Meaning that the change from disordered to ordered motion will be sudden. However, strong finite-size effects could even out this effect.

Grossmann et al. [6] presents a model for both ordered motion and vortex formation. Their model relies on inelastic collisions between disk shaped agents to promote alignment, and thus ordered movement. By imposing reflecting walls at the boundaries of their system, Grossmann et. al, manages to suppress movement perpendicular to the wall, while maintaining the parallel movement resulting in vortices for circular and square systems.

[1] As in, not on the boundary of the flock

[2] Vectorial noise refers to the problems a single particle may have when attempting to aligning with neighbouring particles

While Quincke rotation was first discovered by Quincke [14], Liao et al. [10] was the first to demonstrate that Quincke rotating beads in confinement could be self-propelled, moving in random directions to the electric field. By making use of a relatively simple experiments based on a Helle Shaw cell, Bricard et al. [2] manages to reproduce the collective behaviour commonly found in nature. In the same article, Bricard et al. [2] also presents the theoretical framework for their system. This article has been the main source of inspiration for this master thesis. With their second article, Bricard et al. [3] focuses more on vortices and vortices formation. The system is largely the same as in Bricard et al. [2], but with some modifications to the boundary conditions.

When discussing active turbulence, it might be sensible to look the bacterial world as a point of reference. In their article, Dunkel et al. [4] investigates the turbulence emerging from a suspension of concentrated *Bacillius subtilis*. They also presents a modified version of the theory presented by Toner and Tu [19]. Meanwhile Petroff et al. [13] use rotating bacteria, of the type *Thovilum majus*, to produce living crystals. The bacteria are attracted to each other by the rotational flow they themselves cause. Combined with their geometrical shape, this results in hexagonal packing and thus crystal like structure.

Yeomans [23] presents a short review article for the interested reader, while a more comprehensive review article is presented by Vicsek and Zafeiris [21].

What Remains to be Done?

Only Bricard et al. [2], Bricard et al. [3] and Liao et al. [10] have so far investigated the Quicke propelled active matter, there is still much to learn from such a system. The other authors have been interested in other systems, but can still provide a reference point for further investigations.

1.2 Objectives

The main objectives of this Master's project are

1. Develop an experimental set-up for investigating Quincke rotation, and Quincke induced self-propulsion.

2. Collect data on collective behaviour and compare results with other sources

1.3 Limitations

This study will be a mostly qualitatively study. While it would be interesting to present an theoretical framework for the observed collective motion, it would simply be beyond the scope of the thesis. As one might expect from complex non-linear non-equilibrium systems, doing so could prove to be both difficult and time consuming. Similarly this thesis will not present any new or modified theoretical framework for collective motion as a whole, instead relying on Vicsek and Zafeiris [21]. The experiments and related procedures were time consuming, to the point that only a limited number of experiments could be conducted, leaving caps in the parameter values that could not be investigated. The most time consuming aspect of the experiments, was to reduce pinning between particles and electrodes (which were reused several times). This required developing a suitable procedure for electrode cleaning. While continuously improved, the systems were never perfectly cleaned. This resulted in some pinning for our system, particularly for slow moving particles. The particles used were not completely spherical, sometimes even having significant deformities. These deformities promotes circular movement for individual particles not related to flocking dynamics.

1.4 Approach

This process is designed to be an iterative process. The experiences made during the master project autumn 2014, combined with the published work of Bricard et al. [2], forms the basis for experimental method in this thesis. The system used to investigate Quincke induced collective motion, will be a simplified version of the system used by Bricard et al. [2][3]. The experimental procedures are changed continuously, to improve the results and reduce wear and tear on equipment.

[3] Bricard et al. [2] uses a racetrack shaped confinement for the quincke rollers, but from previous experience such a system is susceptible to strong edge-flow effects.

1.5 Structure of the Report

The rest of this report is organized as follows. Chapter 2 gives an introduction to some of the theoretical background, chapter 3 presents the methodology and procedures being followed. Chapter 4 presents the results obtained and compares them to previous work. Finally chapter 5 presents the final summary and discussion, with recommendations for further work.

Chapter 2

Theory

This section aims to provide some background theory relevant for this paper. Firstly, we will attempt to present theory relevant for the field of active matter as a whole. Then the attention will be turned towards Quincke rotation and its dynamics.

2.1 Active matter

2.1.1 The Vicsek Model

Vicsek et al. [22] was the first to establish a quantitative model for describing the collective behaviour of active matter. This model is now often referred to as the Vicsek Model[7] or the Standard Vicsek Model[21]. The 2D version goes as follows; a system of self- propelled particles are moving at constant velocity v_0, a single particle will, in accordance with Reynolds [15], attempt to move in the general direction of the of its neighbours. The neighbours are defined as all the particles within a radius of R. Based on this, Vicsek and Zafeiris [21] presents the following equations of motion for the single particle.

$$\mathbf{v}_i(t+1) = v_0 \frac{\langle \mathbf{v}_j(t) \rangle_R}{|\langle \mathbf{v}_j(t) \rangle_R|} + \eta \tag{2.1}$$

$$\mathbf{x}_i(t+1) = \mathbf{x}_i(t) + \mathbf{v}_i(t+1) \tag{2.2}$$

Where $\mathbf{v}_i(t)$ and $\mathbf{x}_i(t)$ is the velocity and position, respectively, of the particle i at time t. The $\langle ... \rangle$ expression refers to averaging of velocities of all neighbouring particles within a circle of radius R. The term $\frac{\langle \mathbf{v}_j(t) \rangle_R}{|\langle \mathbf{v}_j(t) \rangle_R|}$, therefore returns the general direction of movement for local group. The final term, η, represents an perturbation, or an error. This perturbation results from an error that a single particle may have when trying to determine the direction of its neighbours. This is equivalent to the *vectorial noise* described by Guillaume and Chaté [7], but the noise could arise from other sources as well such as boundary conditions.

The direction of movement for the particle within the circle of radius **R** is determined by the angle θ_i. Again, based on this Vicsek and Zafeiris [21] presents the following compact equations of motion for the direction of the particle.

$$\theta_i(t) = \arctan\left[\frac{\langle v_{j,x} \rangle_R}{\langle v_{j,y} \rangle_R}\right] \tag{2.3}$$

$$\theta_i(t+1) = \theta i(t) + \Delta_i(t) \tag{2.4}$$

where $\Delta_i(t)$ now represents the perturbations, while $v_{j,x}$ and $v_{j,y}$ denotes the x and y components of the velocity v_j. It is important to note that the only parameters in the Vicsek Model are the particle density ρ, the absolute velocity v_0 and the perturbation,η.

When measuring the degree of order in an system, the Vicsek Model presents the order parameter ϕ which is defined as follows:

$$\phi \equiv \frac{1}{N \cdot v_0} \left| \sum_{i=1}^{N} \mathbf{v}_i \right| \tag{2.5}$$

here, N is the number of particles in the entire system. This means that a perfectly ordered system will have $\phi = 1$, and conversely a perfectly disordered system will have $\phi = 0$.

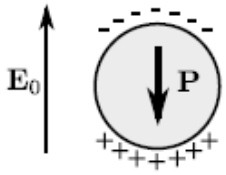

Figure 2.1: This the charge build up experienced by an spherical particle, and the resultant dipole. Figure taken from [2]. Keep in mind that the charge relaxation time of the particle is here greater than the charge relaxation time for the external fluid

2.2 Quincke induced collective motion

2.2.1 Single Quincke Roller

The following theory is based on Bricard et al. [2] and later on Turcu [20]. When an insulating particle is suspended in an conductive liquid[1], and is subjected to an external electric field $\mathbf{E}_0 = E_0\hat{z}$, then there will be a charge build up on the surface. See figure 2.1. This charge build up can be described as an surface charge distribution following:

$$q_s = (\varepsilon_l \mathbf{E}^l - \varepsilon_p \mathbf{E}^p) \cdot \hat{r}|_{r=a} \tag{2.6}$$

q is the surface charge, $\mathbf{E}^i$ and ε_i are the electrostatic field and the dielectric constant of medium i respectively. The indexes l and p are used to indicate the liquid and the particle. a is the radius of the particle. The charge distribution crates an dipole $\mathbf{P}$

$$\mathbf{P} = \int_0^a q_s \hat{r}\, \mathrm{d}s^2 \tag{2.7}$$

The surface current will be conserved in according to $\partial t q_s + \nabla_s \mathbf{j}_s = 0$. Here $\nabla_s = (\mathbf{I} - \hat{\mathbf{r}}\hat{\mathbf{r}})$ is the surface divergence operator, and $\mathbf{j}_s$ is the surface current. There are two contributions to $\mathbf{j}_s$, these are the ohmic conductance $\mathbf{j}_o = \sigma\mathbf{E}$ and the rotational advection current $\mathbf{j}_r = q_s\Omega \times a\hat{r}$. This gives the total surface current $\mathbf{j}_s = \sigma\mathbf{E} + q_s\Omega \times a\hat{r}$. Combined with eq. (2.7), one gets the following dynamical equation for $\mathbf{P}$

[1] $\tau_l < \tau_p$, where $\tau_i = \varepsilon_i/\sigma_i$. And ε_i and σ_i is the permittivity and the conductivity of medium i. The index p indicates particle while l represents the liquid.

$$\frac{d\mathbf{P}}{dt} + \frac{1}{\tau}\mathbf{P} = -\frac{1}{\tau}2\pi\varepsilon_0 a^3 \mathbf{E}_0 + \Omega \times (\mathbf{P} - 4\pi\varepsilon_0 a^3 \chi^{\infty}\mathbf{E}_0) \tag{2.8}$$

where $\chi^{\infty} = \frac{\varepsilon_p - \varepsilon_l}{\varepsilon_p + 2\varepsilon_l}$ is the high frequency polarisability, and $\tau = \frac{\varepsilon_p + 2\varepsilon_l}{2\sigma_l}$ is the Maxwell-Wagner time.

There are two contributions to the polarization vector $\mathbf{P} = \mathbf{P}^{\infty} + \mathbf{P}^{q_s}$. The first term, $\mathbf{P}^{\infty} = 4\pi\varepsilon_0 a^3 \chi^{\infty}\mathbf{E}_0$, is due to the dielectric polarization of the particle. This term can be considered static, or instantaneous. The second term, $\mathbf{P}^{q_s}$, results from the distribution of surface charges across the particle. This term is dynamical in the sense that should the particle rotate, then the displacement of surface charges will result in a new $\mathbf{P}^{q_s}$. This, in turn, creates an electric torque, $\mathbf{T}_E$, acting on the particle. When this torque is balanced by the viscous torque, $\mathbf{T}_\eta$, the particle will undergo stable rotational motion. The static and dynamical terms will compete with each other, the static term will be dominant when the particle is at rest. Any perturbation of the particle will favour the dynamic term. See figure 2.2

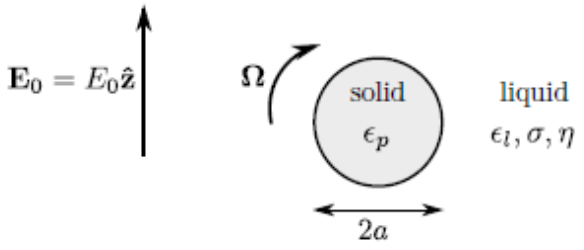

Figure 2.2: This figure demonstrates a rotating particle due to an initial perturbation. ε is the permittivity, σ is the conductivity and η is the viscosity. The index p indicates the particle, the rest belongs to the liquid. Figure taken from[2]

From eq. (2.8), Bricard et al. [2] determine that the critical field required for Quincke rotations is given by:

$$E_Q = \left[4\pi\varepsilon_l a^3(\chi^{\infty} + \frac{1}{2})\mu_r\tau\right]^{-1/2} \tag{2.9}$$

with $\mu_r = (8\pi\eta a^3)^{-1}$ is a rotational friction coefficient. It should be noted that while eg. (2.9) includes an a^3, it is cancelled by the a^{-3} term in μ_r. This means that the critical field does not depend on the size of the suspended particle. Furthermore, the angular velocity of the rotation

is given as:

$$\Omega = \frac{1}{\tau}\sqrt{\frac{E_0^2}{E_Q^2} - 1} \tag{2.10}$$

On its own, a rotating unbounded particle will not have translational movement. It will need something to push against for it to have net force acting on it. By introducing an electrode surface, Bricard et al. [2] calculates that the translational velocity is:

$$v_0 = \frac{a\tilde{\mu}_t}{\mu_r \tau}\sqrt{\frac{E_0^2}{E_Q^2} - 1} \tag{2.11}$$

where the translational friction coefficient, $\tilde{\mu}_t$, is related to the effect of the electric torque, $\mathbf{T}_E$, on the translational velocity. This quantity is not fully controlled, but Bricard et al. [2] finds that $\frac{a\tilde{\mu}_t}{\mu_r \tau} \approx 2\text{mm} \cdot \text{s}^{-1}$ for a system with $a = 2.4\mu\text{m}$, $\tau \approx 1\text{ms}$, $\eta \approx 2\text{mPa} \cdot \text{s}$

Determining the critical field

Bricard et al. [2] do not explicitly show the calculations for determining E_Q. However, calculations based on Turcu [20] is shown below.

A perturbed particle will experience an electrical torque:

$$\mathbf{T}_E = \mathbf{P} \times \mathbf{E}_0 \tag{2.12}$$

where, as before, the electric field in the rest system can be described by:

$$\mathbf{E}_0 = E_0 \hat{z} \tag{2.13}$$

In a rotating coordinate system at rest with respect to the particle, the electric field can instead be expressed as:

$$\mathbf{E}_0 = \mathfrak{Re}\left[E_0(\hat{z} - i\hat{x})e^{-i\Omega t}\right] \tag{2.14}$$

The unit vectors $\hat{z}$ and $\hat{x}$ define the plane in which the rotation takes place. The dipole is given as:

$$\mathbf{P} = Re\left[4\pi\varepsilon_l a^3 \frac{\tilde{\varepsilon_p} - \tilde{\varepsilon_l}}{\tilde{\varepsilon_p} + 2\tilde{\varepsilon_l}} E_0(\hat{z} - i\hat{x})e^{-i\Omega t}\right] \tag{2.15}$$

with complex permittivities $\hat{\varepsilon}_p = \varepsilon_p - i\frac{\sigma_p}{\Omega}$ and $\hat{\varepsilon}_l = \varepsilon_l - i\frac{\sigma_l}{\Omega}$ Inserting eq. (2.14) and eq. (2.15) into eq. (2.12), results in the following expression for the torque, $\mathbf{T}_E$:

$$T_E = 9 \cdot 4\pi a^3 \varepsilon_l E_0^2 \frac{\varepsilon_r - \sigma_r}{(\varepsilon_r + 2)(\sigma_r + 2)} \frac{X}{X^2 + 1} \tag{2.16}$$

with $\varepsilon_r = \frac{\varepsilon_p}{\varepsilon_l}$, $\sigma_r = \frac{\sigma_p}{\sigma_l}$, $X = \Omega\tau$ and $\tau = \frac{\varepsilon_p + 2\varepsilon_l}{\sigma_p + 2\sigma_l}$ is the Maxwell Wagner time.
The viscous forces in the suspending liquid will try to counteract any rotation. The viscous torque, T_η, acting on the particle is:

$$T_\eta = -6 \cdot 4\pi a^3 \eta\Omega \tag{2.17}$$

This leads to the following dynamical equation of motion:

$$I\frac{d\Omega}{dt} = T_E + T_\eta \tag{2.18}$$

where I is the moment of inertia for the particle.
By inserting eq. (2.16) and eq. (2.17) into (2.18), and simplifying, one ends up with the following dimensionless equation:

$$\frac{dX}{dt} = CX\left(\frac{p}{X^2 + 1} - 1\right) \tag{2.19}$$

with $C = \frac{6 \cdot 4\pi a^3}{I}$, $p = \frac{E_0^2}{E_Q^2} sgn(\varepsilon_r - \sigma_r)$ and $E_Q = \sqrt{\frac{2\eta(\sigma_r + 2)^2}{3\varepsilon_l \tau_l |\varepsilon_r - \sigma_r|}}$

Excluding the conductivity of the particle, yields in the following simplification:

$$p = \frac{E_0^2}{E_Q^2} \tag{2.20}$$

$$E_Q = \sqrt{\frac{8\eta}{3\varepsilon_l \tau_l \varepsilon_r}} \tag{2.21}$$

where eq. (2.21) is now equivalent to eq. (2.9)

Using simple stability analysis, one finds two stable state solutions for eq. (2.19) (i.e when $\frac{dX}{dt} = 0$):

$$X_1 = \quad 0 \tag{2.22}$$

$$X_2 = \quad \pm\sqrt{p-1} \tag{2.23}$$

Where (2.23) is rotational velociy of the particle, and combined with $X = \Omega\tau$ it can be rewritten into eq. (2.10). The pluss-minus sign indicates that the rotation can be either clockwise or counter-clockwise. $X_1 = 0$ corresponds to a stable stationary state. But when $E_0 > E_Q$, corresponding to $p > 1$, this stable state disappears and any small pertubation can trigger stable rotational motion instead. The direction of rotation is entirely dependent on the initial pertubation. This conclusion is only valid for $\tau_l < \tau_p$[2]. If this condition is not true, then there would only be one stable state $\Omega = 0$. See Jones [8] for more details regarding the Quincke rotations and an alternative solution to the dynamical equation of motion based on linearisation.

2.2.2 Interaction with other particles

When several particles are introduced to the system, they will interact with one another both electrostatically and through hydrodynamic processes. The surface charge distribution of one particle will interfere with the surface charge distribution of another. Moreover, the dipole on of any particle will create an image dipole in nearby surfaces which also affect the other particles. Additionally, when one particle move it will cause the fluid around it to move, which will affect other particles by creating an external flow field $\mathbf{u}_\parallel$. By using an modified version of eq. (2.8), Bricard et al. [2] is able to prove that:

$$\frac{d\theta}{dt} = \frac{a}{\tau v_0}\frac{\tilde{\mu}_s}{\tilde{\mu}_t}\hat{\mathbf{p}}_\perp \cdot_z \partial \mathbf{u}_\perp|_{z=0} - \frac{v_0}{a}\frac{\mu_r}{\mu_t}\left(\frac{\mu_\perp}{\mu_r} - 1\right)\hat{\mathbf{p}}_\perp \cdot \frac{\delta \mathbf{E}_\parallel}{E_0} + \frac{a\tilde{\mu}_r}{\tau\mu_r}\hat{\mathbf{p}}_\perp \cdot (\mathbf{P}\cdot\nabla)\frac{\delta \mathbf{E}_\parallel}{E_0} \tag{2.24}$$

where θ is the direction of the plane component of the polarization direction. And $\hat{\mathbf{P}}_\perp = -\sin\theta\hat{\mathbf{x}} + \cos\theta\hat{\mathbf{y}}$. $\tilde{\mu}_s$ and $\mu_\perp$ are mobility coefficients related to the external field flow and the rotation of

[2] where τ_p and τ_l is the charge relaxation time for the particle and the liquid respectively.

the particles respectively. $\hat{\mathbf{u}}$ and $\delta\mathbf{E}_{\parallel}$ refers to the inhomogeneities in the $\mathbf{E}_{\parallel}$ field. $\tilde{\mu}_r$ is the rotational friction coefficient for another interacting particle. From eq. (2.24), it can be seen, in the first term on the left hand side, that $\hat{\mathbf{p}}_{\perp}$ will seek to align with the external flow field. This means that the particles will seek to align themselves with the external field. Bricard et al. [2] argues that the contributions from field heterogeneities, produced by the interfering charge distributions, are small and can be ignored. The translational velocity of the rotating particles will therefore remain the same as in eq. (2.11).

While the particles will tend to align themselves in the same direction, it will take a certain density, or area fraction ϕ, of rollers for this tendency to create an homogeneous group of particles.Bricard et al. [2] presents this critical density, ϕ_c, as:

$$\phi_c = \frac{\tau D_r}{\alpha} \tag{2.25}$$

where D_r is the rotational diffusion coefficient of the rotating particles. And α is defined as:

$$\alpha = \frac{3}{2}\tilde{\mu_s} + \frac{3}{8}(\frac{\mu_{\perp}}{\mu_r} - 1)(\chi^{\infty} + \frac{1}{2})(1 - \frac{E_Q^2}{E_0^2}) \tag{2.26}$$

α is related to the hydrodynamic alignment of particle interactions. An polar ordered phase, that is when every particle is aligned, would be a clear case of collective movement.

Chapter 3

Methods and Procedures

3.1 Set-up

The set-up consists of a simple Helle-Shaw cell as seen in fig (ISERT FIG). The cell is made of two Sigma-Aldritch ITO-coated glass slides sandwiching a double layered Scotch tape. A rectangular 1.5cm$x$5.0cm chamber was cut out from the tape using a Swann-Mosrton disposable scalpel. The ITO slides were turned inward towards the cell chamber with respect to their electrode surface. The chamber is then filled with a suspension of plastic beads in a AOT[1]/hexadecane solution. Beads made of PMMA (polymethyl methacrylate) and PE (polyethylene) were used separately. The size of the beads was varied between a radius $a = 20\mu$m to $a = 85\mu$m. The AOT salt concentration also varied in order to control conductivity of the liquid, which in turn determined the speed of Quincke rotations. However, most experiments were conducted using a 0.15moll^{-1} salt concentration. The electrodes are then connected to an external high voltage source, here LKB Biochrom 2103 Power Supply. The system was investigated using a Zeiss Stemi 2000-C stereo microscope connected to a Canon EOS 650D camera. Some systems were investigated more closely using a Leitz Wetzlar Orthoplan microscope connected to a Panasonic DMC-GH4 camera.

[1] Another name for AOT salt is dioctyl sodium sulfosuccinate

3.2 Methods

The cell was assembled by first applying the tape to the bottom electrode. The chamber was then cleaned using compressed air. The fluid would then be injected into the chamber and slightly overfill it so that the fluid surface would reach above the chamber walls. The top ITO electrode could then be slid into place, pushing away excess fluid. An important point, while a double sides tape was used as chamber walls, the separation paper was never removed, allowing the upper ITO slide to be moved along the surface independently. The system was then held together using ordinary clothes-pins. When the system was fully assembled, it was given some time to allow the plastic beads time to sedimentate. The cell would then be connected to the voltage supply, the applied voltage was increased until some form of collective behaviour could be observed. Most observations were done using the Canon EOS 650D Camera because of its remote shooting capabilities. The 4k resolution camera Panasonic DMC-GH4 was installed to investigate systems on a smaller scale.

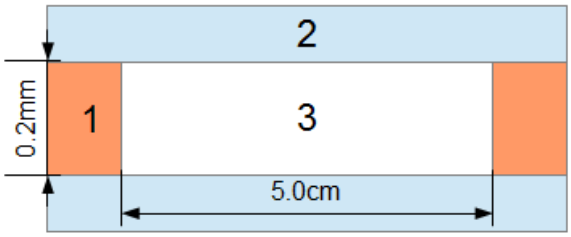

Figure 3.1: This figure show cross section of the cell, seen from the side, used for the experiments. 1. The cell walls are made of double sided scotch tape. 2. ITO slide electrode. 3. The cell chamber for the suspended particles.

3.3 Preparation and cleaning

The methods of preparation for the system were constantly modified and changed to improve the quality of the system, outlined below is the final standardized method for preparing the system. When preparing the AOT/Hexadecane solution it was discovered that the AOT salt was hydrated 2.1%. Since the water might increase the conductivity, the salt was dehydrated in a heat cabinet for a few days before use. From that point on, the solution could be prepared to a

high degree of accuracy, usually to the third significant number using a OHAUS Analytical Plus digital weight.

Between use the ITO slides were cleaned using the following procedure. First the ITO slides would individually be given a supersonic bath at 50 degC in a plastic bottle containing 2% diluted Hellmanex III detergent. After 30min in the bath, the slides were transferred to another plastic container filled with distilled water. After another 30min the slides would be taken out from the bath and rinsed with ethanol and then polished using fine optical paper from Edmund Industrial Optics. Once the polishing was done, compressed air was used to remove any paper fibres stuck to the surface.

3.4 Weaknesses and Limitations

As was mentioned earlier, the systems used did not reach the desired level of cleanliness. Detergents are typically slow acting, and 30min might not have been enough. Letting the ITO slides stay in the bath over the night, might have been preferable. Polishing the ITO slides after using the detergent could be counter productive. While the degree of pinning went down, some paper fibres got stuck and could not be removed with the compressed air. Paper fibres became the most commonly observed foreign objects in the system. The glue in the scotch tape may contain a broad spectrum of different chemicals, that could leak out into the system. Their effect is currently unknown. Due to the way that the system had to be assembled with the fluid inside, air bubbles could sometimes form on the surface of the suspension fluid when the top ITO slide was put in place. The air bubbles typically interfered with the movement of the plastic beads by adding another surface for the beads to interact with. Similarly because of the assembling process the life span varied significantly. It could last 1 hour or 3 days before air bubbles would start to form along the edges. The lifespan was dependent on how evenly the tape had been applied to the bottom electrode and the evenness of the placement of the clothes-pins. The system exhibited a high degree of pinning, by courtesy of Dr. Jakko Timonen we found a way to test it. The cell was put on an incline with no voltage applied. The beads should therefore only experience gravitational pull, and thus move down the incline. However some particles get stuck, seemingly at random. And others never seem to move see fig: 3.2. This effect is probably

due to the presence of foreign objects on the surface of the electrodes.

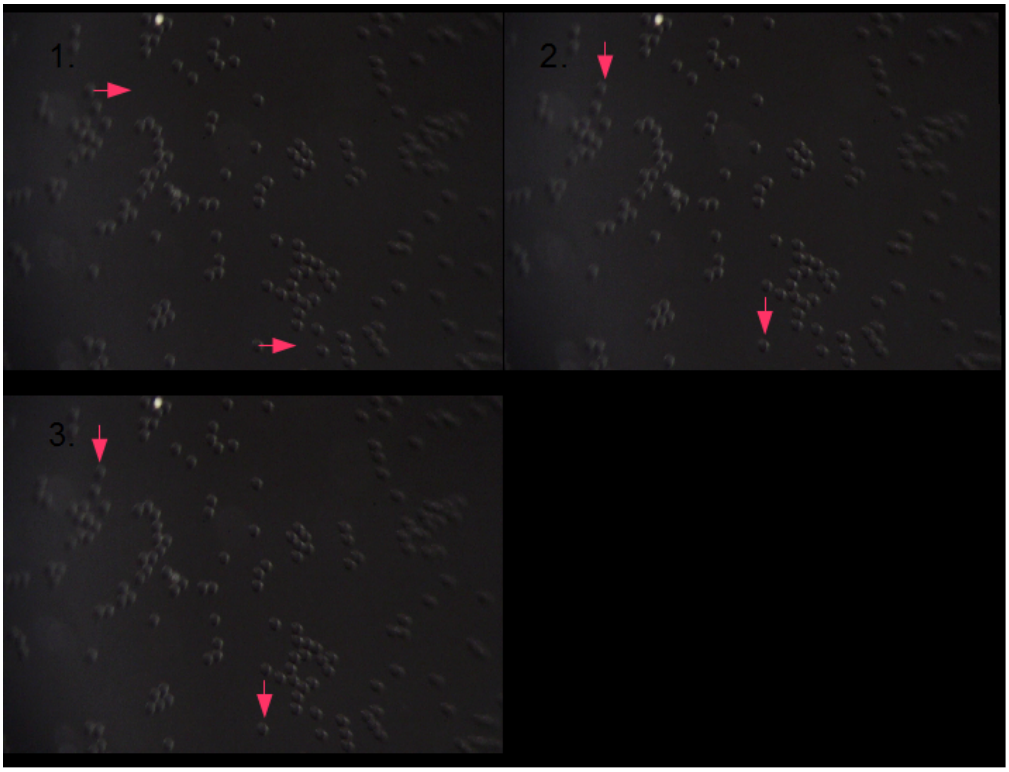

Figure 3.2: Inclined cell, the cell is tilted towards the left. 1. Some initial movement can be seen, marked with red arrows. 2. The moving particles comes to a stop. 3. Even some time after, the particles refuses to move futher down the slope. Particle type: PMMA, particle size radius= 40μm. The pictures are arranged in chronological order

Chapter 4

Results

In this chapter we will present some of the qualitative data gathered and attempt to connect it with previous works. When conducting the experiments, it was important to confirm that the Quincke rotors were, in fact, rotating. On closers inspection with the orthoplan microscope, it was discovered that the 85μm had visible irregular internal structures. By using these internal structures as a reference point, and applying a field close to the critical field E_Q, it became possible to visibly see the rotation taking place. See fig: 4.1 for the results.

4.1 Active turbulence

Most cases of turbulence arose from multiple vortices forming, as in Figs. 4.3, 4.4, 4.5 and 4.6. However, at low particle concentrations and with the electric field being just above the citical point, one could observe collective motion without order, as seen in Fig. 4.2. This is remotely similar to the bacterial turbulence reported byDunkel et al. [4].

4.2 Vortex formation

Vortices were frequently formed in systems if the concentration exceeded a certain threshold value. Fig. 4.3 and Fig. 4.4 both provides good examples of vortex formation. Fig. 4.5 is taken from the same system as Fig. 4.4, but image contrast has been improved. The vortices were commonly observed in pairs, or multiples as seen in Fig. 4.4, rotating in opposite directions

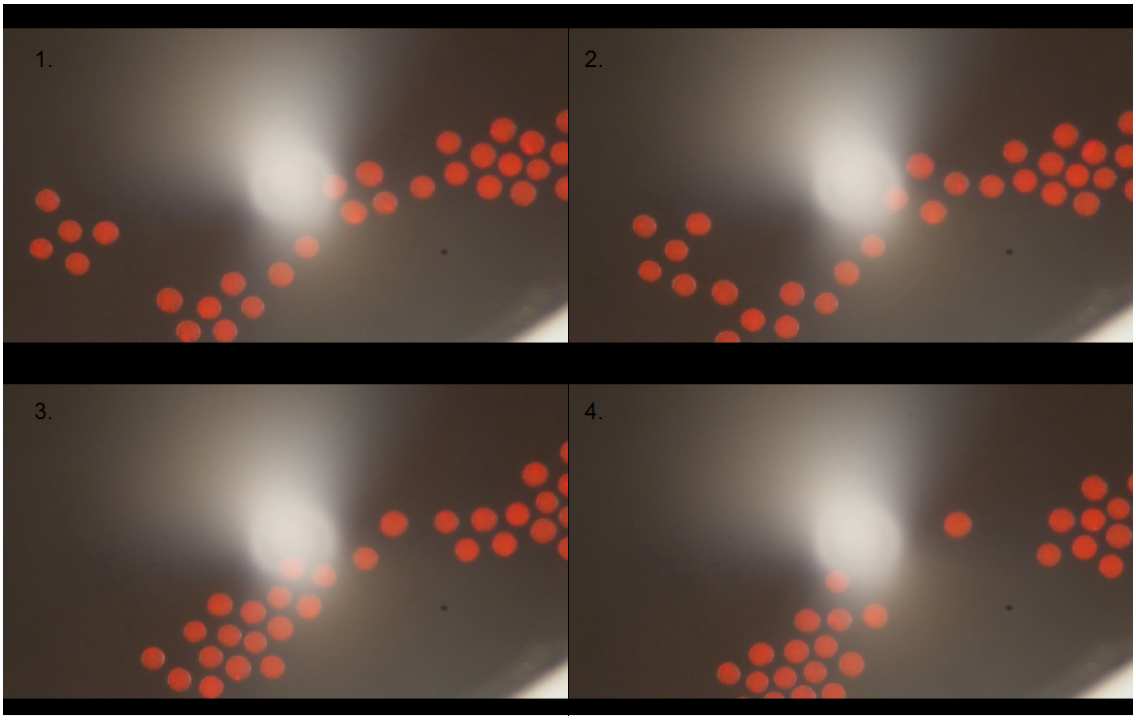

Figure 4.1: Rotating particles: Particle type: PE, particle radius = 85μm. AOT salt concentration is 0.15moll[1]. 1. A small group of particles are entering the field of view from the left. 2. The group moves closer to the larger group on the right. 3. The two groups have joined together. 4. The new group is split in two in a north south direction. By looking at the change in the visible internal structure of the particles, it can be determined that they are rotating. The pictures are sorted chronologically

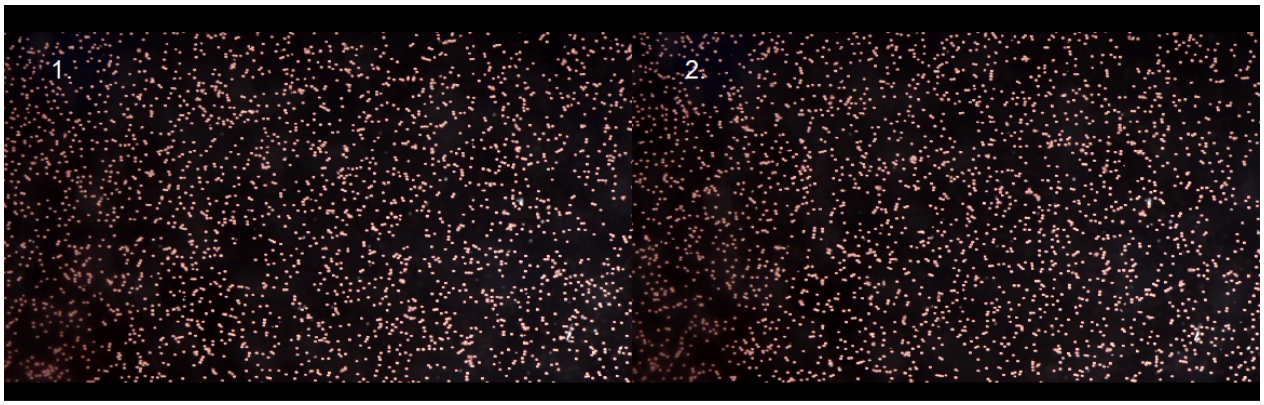

Figure 4.2: Turbulence: Particle type: PE, particle radius $a = 50\mu$m, salt concentration 0.30moll^{-1}, particle concentration is 0.0.09% measured in terms of weight percentage. The electric field is $E = 1240\text{V/mm}$

to each other. Fig 4.6 shows the formation of a voretex When investigating Quincke induced collective motion, Bricard et al. [3] also reports observing vortices. However, in their case they only observe one vortex per system, with the vortex occupying most of the space. The vortices are, however, qualitatively consistent with the simulations presented by Grossmann et al. [6]

4.3 Living Crystals

The living crystals may be the most fascinating phenomenon that was observed over the course of this master project. While investigating the phase transition from disordered motion to ordered motion it was discovered under certain circumstances these crystal formations could form. In Fig. 4.7 it can be clearly seen that the crystals move, disintegrate and reform. It should be noted, however, that this system was not prepared like outlined in chapter 3. Instead of using ethanol to rinse the ITO slides, acetone was used. Furthermore the ITO slides were not polished with the optical paper. Despite becoming the main focus of investigation once discovered, it proved difficult to reproduce the results. In Fig. 4.1 one can see a tendency to form hexagonally packed groups, these groups would, if they were packed more closely, resemble small crystals. The visual look of Fig. 4.7 is similar to the living crystal systems presented by both Palacci et al. [11] and Petroff et al. [13]. Fig. 4.8 was the first observation of living crystals made with this system. It can be concluded that the living crystal, at least for the Quincke rotor system, represents a sensitive solution to flocking dynamics.

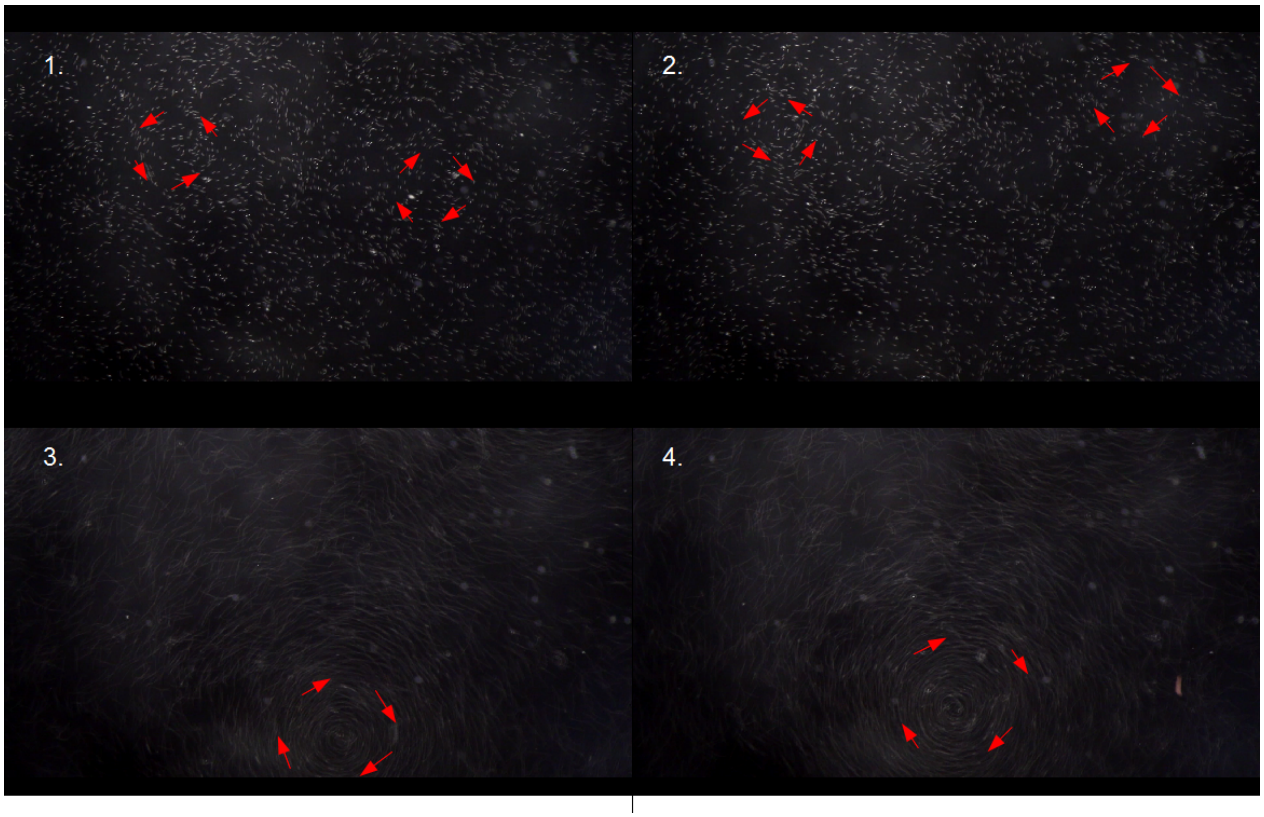

Figure 4.3: Vortices: Particle type: PMMA, particle radius $a = 30\mu$m, salt concentration 0.075moll^{-1}, particle concentration is 0.4% measured in terms of weight percentage. In pictures 1. and 2. the electric field is $E = 1420\text{V/mm}$, and in picture 3. and 4. the electric field is $E = 3210\text{V/mm}$. Red arrows are included in the two first pictures to show more clearly that the spirals are there.

Most attempts to recreate the living crystals ended up like Fig. 4.9. The particles pack themselves together with increasing field strength, but once the critical E_Q is passed, the clusters begins to evaporate. Interestingly Fig. 4.9 is very similar to particle behaviour due to the Lennard-Jones potential shown in Stillinger and Stillinger [17].

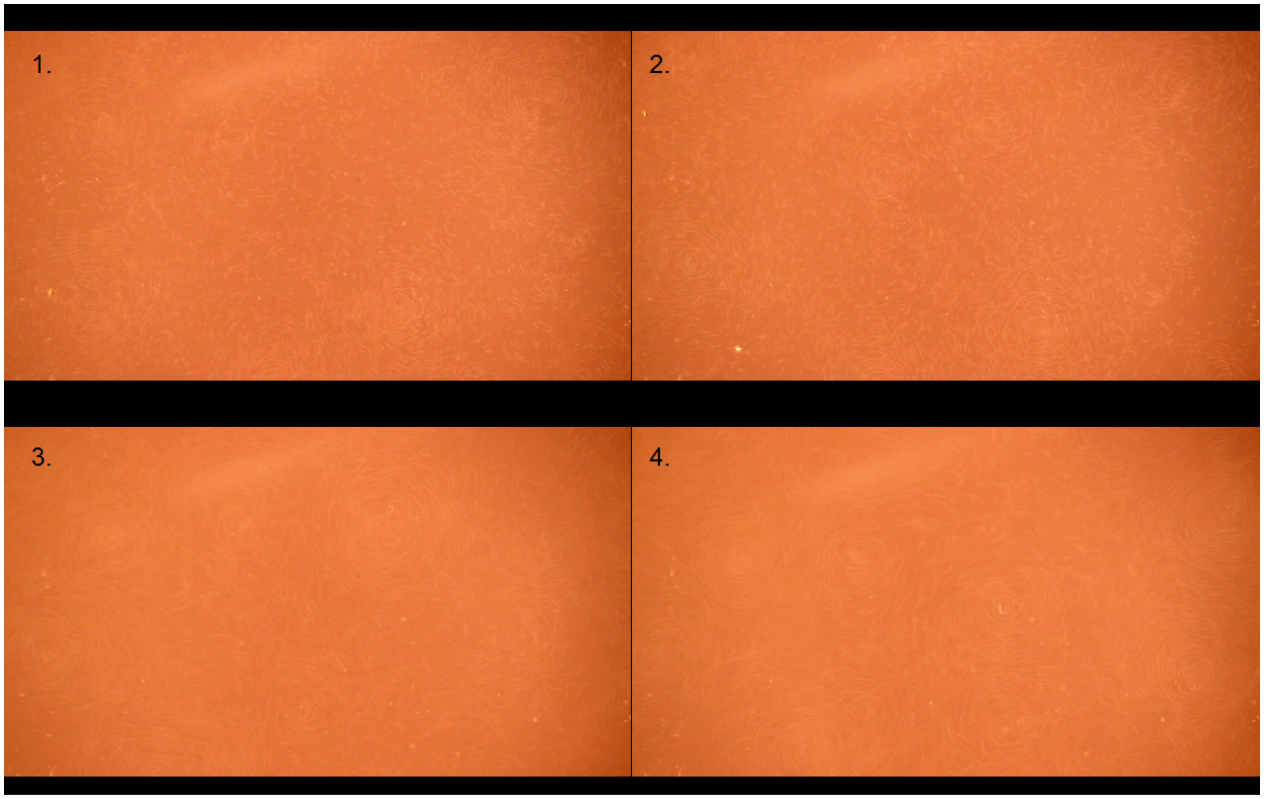

Figure 4.4: Vortices: Particle type: PMMA, particle radius a = 30μm, salt concentration 0.15moll^{-1}. In pictures 1. and 2. the electric field is E = 1750V/mm, and in picture 3. and 4. the electric field is E = 2500V/mm

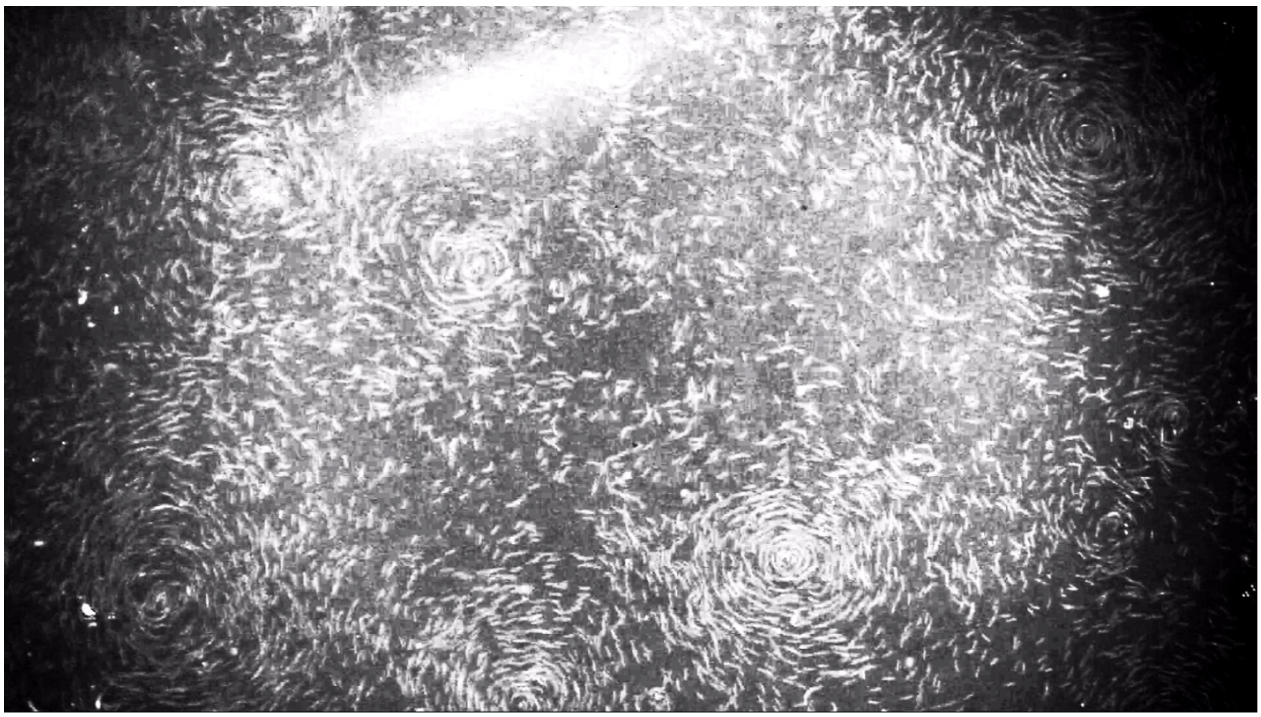

Figure 4.5: Vortices: Particle type: PMMA, particle radius $a = 30\mu$m, salt concentration 0.15moll^{-1}. The electric field is $E = 1750\text{V/mm}$. Experiment: Tommy F. Kristiansen, Image analysis: Paul Dommersnes.

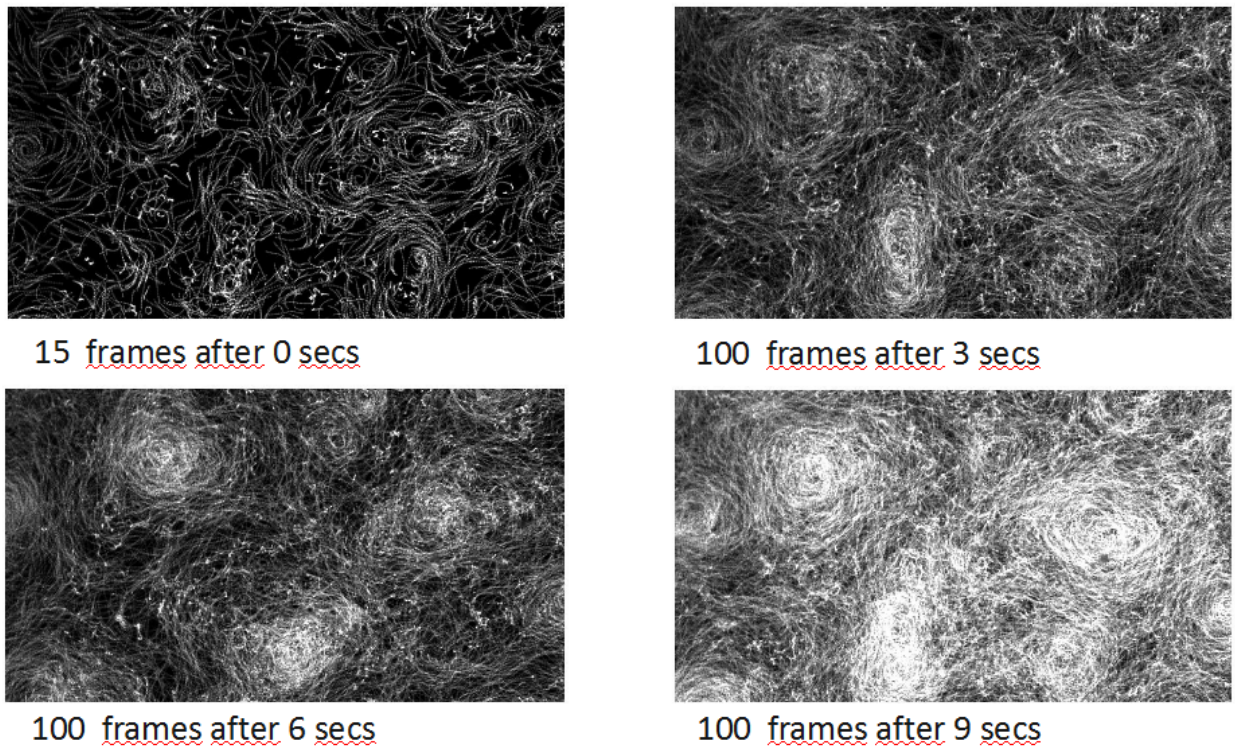

Figure 4.6: Vortices: Particle type: PMMA, particle radius $a = 30\mu$m, salt concentration 0.15moll^{-1}. The electric field is $E = 1750\text{V/mm}$. The vortices appear more clearly when several images are superimposed to show the trajectory of the particles. Experiment: Tommy F. Kristiansen, Image analysis: Paul Dommersnes.

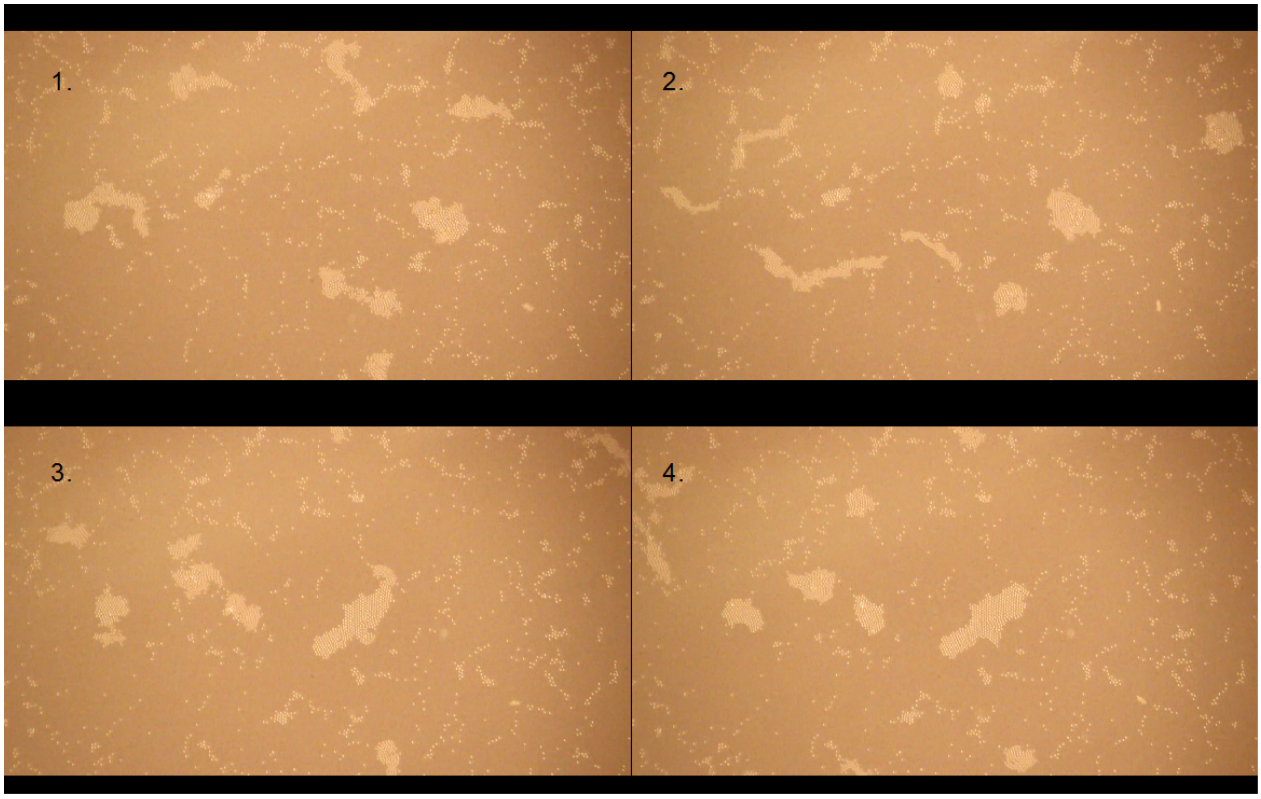

Figure 4.7: Living Crystals: Particle type: PMMA, particle radius $a = 40\mu$m. Salt concentration 0.15moll^{-1}. Electric field strength $E = 1375V/mm$. The pictures 1.-4. displays crystal like formations constantly moving, stopping and reshaping. The pictures are ordered chronologically. The ITO slides in this system were rinsed in acetone instead of ethanol, and they were not polished before use.

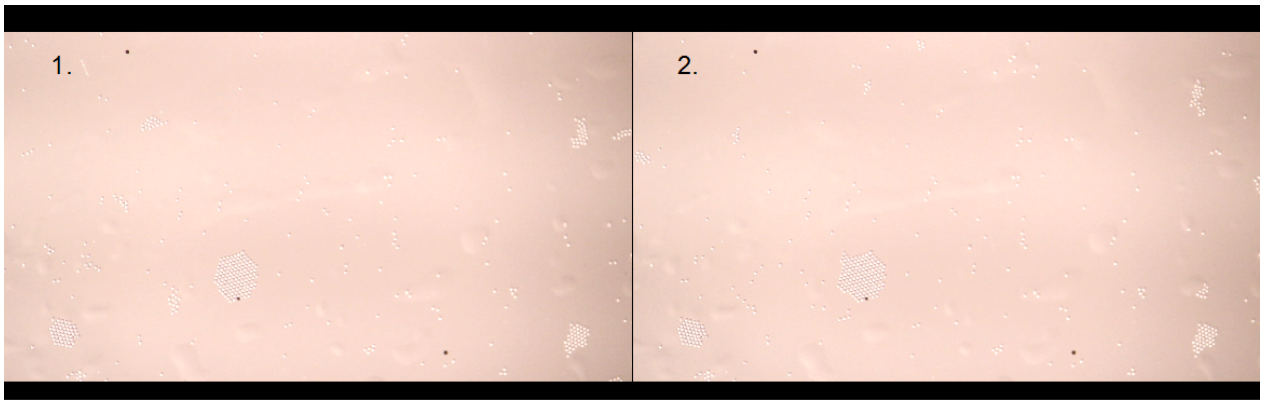

Figure 4.8: Living Crystals: Particle type: PMMA, particle radius $a = 40\mu$m. Salt concentration 0.15moll^{-1}. Electric field strength $E = 1750V/mm$. The pictures 1.-2. displays crystal like formations constantly moving, stopping and reshaping. The pictures are ordered chronologically. The ITO slides in this system were rinsed in acetone instead of ethanol, and they were not polished before use.

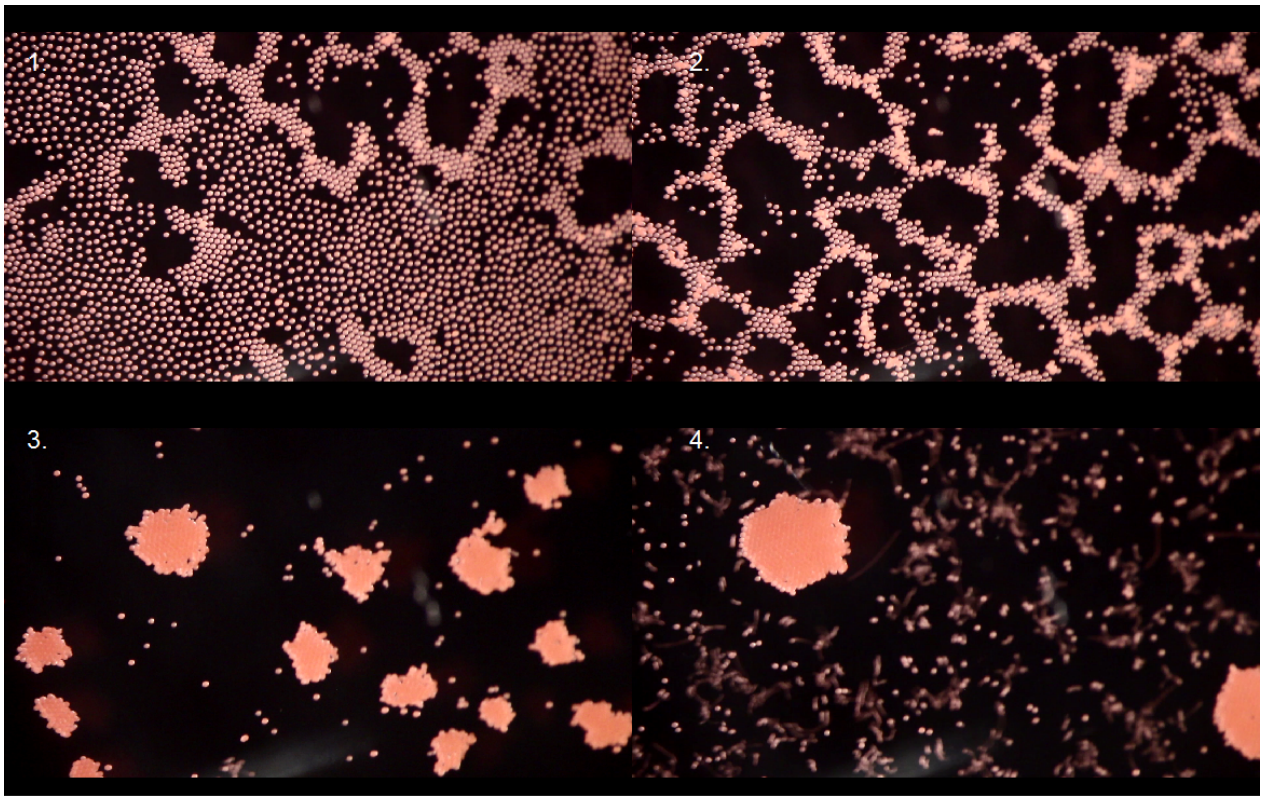

Figure 4.9: Attempt at making Living Crystals: Particle type: PE, particle radius $a = 50\mu$m. Salt concentration 0.30moll^{-1}. Electric field strength was increased steadily from $E = 1000V/mm$ to $E = 4500V/mm$. If one feels particularly inclined towards generosity, one could regard pictures 3.-4. as living crystals.The pictures are ordered chronologically.

Chapter 5

Summary and Recommendations for Further Work

5.1 Summary and Conclusions

When comparing with previous work, it seems most reasonable to primarily rely on Bricard et al. [2] and Bricard et al. [3]. It is interesting that [3] only seems to report large system wide vortices, while the system used in this thesis often displayed many small ones. Especially when considering the structural similarities between them. It could be, that the current set-up is simply too unclean, resulting in more sources of perturbation than Bricard et al. [3]. But there is also a difference in scale, Bricard et al. [3] uses $a = 5\mu$m sized PMMA beads, whereas here particles up to $a = 85\mu$m. This difference in scale could change the point of balance between the electrodynamic and hydrodynamic forces, and thus change the overall dynamic. The vortices are qualitatively consistent with the simulations presented by Grossmann et al. [6]. Fig. 4.2 is not seem quite as active as the bacteria presented by Dunkel et al. [4], but the overall movement is remotely similar. The most interesting result from these experiment are the living crystal. It is interesting because it was difficult to achieve, because it is the first case of living crystals in a Quincke experiments and even more interesting when considering that we do not entirely know how to get them again.

5.2 Discussion

The system designed to investigate Qunicke induced collective collective motion, did produce some acceptable results with regards to observed forms of collective behaviour. However, as was proved by Dr. Jakko Timonen, there is room for improvement with regards to pinning in the system. Comparing the collected data with existing sources, creates some interesting problems, especially with regards to the vortices. It is important to note that while it has been difficult to do it consistently, this is the first time living crystals have been observed in a system of Quincke rotating particles. The cleaning procedures can be improved by letting the ITO slides remain in their supersonic detergent bath over several hours, perhaps as mush as a day.

5.3 Recommendations for Further Work

The translational velocity of a hard rotating sphere is given by $v = \Omega \cdot r$, and Ω depends on the electric field strength through eq. (2.10), it might be interesting to plot the velocity against the expected Ω. The idea is to determine if the velocity might be better represented by $v = \alpha \cdot \Omega \cdot r$, where α is an coefficient determined by the surface contact the rotating sphere actually has with the electrode surface. This idea bore fruit from discussions with Paul Dommersnes, but there was not enough time to implement it. However, it is recommended for further work. And could be done in the short term. A more long term goal would be to further investigate living crystals. The aim would be to reduce pinning in the system, through better cleaning procedures, and thus remove a source of perturbation in the system.

Bibliography

[1] I. S. Aranson, D. Volfson, and L.S Tsiming. Swirling motion in a system of vibrated elogated particles. *Physical Review E*, 75:051301, 2007.

[2] A. Bricard, J-B Caussin, N. Desremaux, O Dauchot, and D. Bartolo. Emergence of macroscopic directed motion in populations of motile colloids. *Nature*, 503(7474):95–98, November 2013.

[3] A. Bricard, J-B. Caussin, D. Das, C. Savoie, V. Chikkadi, K. Shitara, O. Chepizhko, F. Peruani, D. Saintillan, and D. Bartolo. Emergent vortices in populations of colloidal rollers. *Nature Comminications*, 6(7470), 2015.

[4] J. Dunkel, S. Heidenreich, K. Drescher, H. H. Wensink, M. Bär, and R. E. Goldstein. Fluid dynamics of bacterial turbulence. *Physical Review Letters*, 110(228102), 2013.

[5] J. Gachelin, A. Rousselet, A. Lindner, and E. Clement. Collective motion in an active suspension of *Escherichia coli* bacteria. *New Journal of Physics*, 16:0250003, 2014.

[6] D. Grossmann, I.S Aranson, and E. Ben Jacob. Emergence of agent swarm migration and vortex formation through inelastic collisions. *New Journal of Physics*, 10(2), 2008.

[7] Grégoire Guillaume and Hughes Chaté. Onset of collective and cohesive motion. *Physical Review Letters*, 92(2), 2004.

[8] Thomas B. Jones. *Electromechanics of Particles*. Cambridge University Press, 1995.

[9] A. Kudrolli, G. Lumay, D. Volfson, and L. S. Tsimring. Swarming and swirling in self-propelled polar granular rods. *Physical Review Letters*, 100:058001, 2008.

[10] G. Liao, I. I. Smalyuhk, J. R. Kelly, O. D. Lavrentovich, and A. Jákli. Electrorotation of colloidal particles in liquid crystals. *Physical Review E*, 72:031704, 2005.

[11] J. Palacci, S. Sacanna, A. P. Steinberg, D. Pine, and P. Chaikins. Living crystals of light-activated colloidal surfers. *Science*, 339(6122):936–940, 2013.

[12] F. Peruani, J. Starruß, V. Jakovljevic, L. Søgaard-Andersen, A. Deutsch, and M. Bär. Collective motion and nonequilibrium cluster formation in colonies of gliding bacteria. *Phys. Rev. Lett.*, 108:098102, 2012.

[13] A. P. Petroff, X-L. Wu, and A. Libchaber. Fast-moving bacteria self-organize into active two-dimensional crystals of rotating cells. *Physical Review Letters*, 114, 2015.

[14] G. Quincke. Ueber rotationen im constanten electrischen felde. *Annalen der Physik*, 295 (11):417–486, 1896.

[15] Craig W. Reynolds. Flocks, herds, and schools: A distributed behavioral model. *Computer Graphics*, 21(4):25–34, July 1987.

[16] I. H. Riedel, K. Kruse, and J. Howard. A self-organized vortex array of hydrodynamically entrained sperm cells. *Science*, 309(5732):300–303, 2005.

[17] F. H. Stillinger and D. K. Stillinger. Expanded solid matter: Two-dimensional lj modeling. *Elsevier: Mechanics of Materials*, 38:958–968, 2006.

[18] I. Theurkauff, C. Cottin-Bizonne, J. Palacci, C. Ybert, and L. Bocquet. Dynamic clustering in active colloidal suspensions with chemical signaling. *Physical Review Letters*, 103:268303, 2012.

[19] J. Toner and Y. Tu. Flocks, herds, and schools: A quantitative theory of flocking. *Physical Review E*, 58(4), 1998.

[20] I. Turcu. Electric field induced rotation of spheres. *J, Phys. A: Math. Gen*, 20:3301–3307, 1987.

[21] T. Vicsek and A. Zafeiris. Collective motion. *Physics Reports*, 514:71–140, 2012.

[22] T. Vicsek, A. Czirók, E. Ben-Jakob, I. Cohen, and O. Shochet. Novel type of phase transition in a system of self-driven particles. *Physical Review Letters*, 75(6):1226–1229, August 1995.

[23] Julia M. Yeomans. Active matter: Playful topology. *Nature Materials*, 13:1004–1005, 2014.